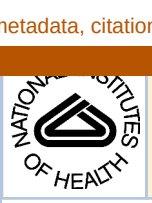

Published in final edited form as:

Int J Dev Neurosci. 2007 June ; 25(4): 233–241.

Insulin-like growth factor-I (IGF-I) inhibits neuronal apoptosis in the developing cerebral cortex *in vivo*

Rebecca D. Hodge[a], **A. Joseph D'Ercole**[b], and **John R. O'Kusky**[a,*]

a *Department of Pathology and Laboratory Medicine, University of British Columbia and the Child & Family Research Institute, 950 West 28th Avenue, Vancouver, British Columbia V5Z 4H4, Canada*

b *Department of Pediatrics, Division of Endocrinology, University of North Carolina at Chapel Hill, Chapel Hill, NC 27599-7220, USA*

Abstract

Increased expression of insulin-like growth factor-I (IGF-I) in embryonic neural progenitors *in vivo* has been shown to accelerate neuron proliferation in the neocortex. In the present study, the *in vivo* actions of (IGF-I) on naturally occurring neuron death in the cerebral cortex were investigated during embryonic and early postnatal development in a line of transgenic (Tg) mice that overexpress IGF-I in the brain, directed by nestin genomic regulatory elements, beginning at least as early as embryonic day (E) 13. The areal density of apoptotic cells (N_A, cells/mm^2) at E16 in the telencephalic wall of Tg and littermate control embryos was determined by immunostaining with an antibody specific for activated caspase-3. Stereological analyses were conducted to measure the numerical density (N_V, cells/mm^3) and total number of immunoreactive apoptotic cells in the cerebral cortex of nestin/IGF-I Tg and control mice at postnatal days (P) 0 and 5. The volume of cerebral cortex and both the N_V and total number of all cortical neurons also were determined in both cerebral hemispheres at P0, P5 and P270. Apoptotic cells were rare in the embryonic telencephalic wall at E16. However, the overall N_A of apoptotic cells was found to be significantly less by 46% in Tg embryos. The volume of the cerebral cortex was significantly greater in Tg mice at P0 (30%), P5 (13%) and P270 (26%). The total number of cortical neurons in Tg mice was significantly increased at P0 (29%), P5 (29%) and P270 (31%), although the N_V of cortical neurons did not differ significantly between Tg and control mice at any age. Transgenic mice at P0 and P5 exhibited significant decreases in the N_V of apoptotic cells in the cerebral cortex (31% and 39%, respectively). The vast majority of these apoptotic cells (>90%) were judged to be neurons by their morphological appearance. Increased expression of IGF-I inhibits naturally occurring (*i.e.* apoptotic) neuron death during early postnatal development of the cerebral cortex to a degree that sustains a persistent increase in total neuron number even in the adult animal.

Keywords

Apoptosis; Caspase-3; Insulin; like growth factor-I; IGF-I; Naturally occurring neuron death; Transgenic mice

1. Introduction

Accumulating evidence indicates that insulin-like growth factor-I (IGF-I) has an important role in brain growth and development. IGF-I is normally expressed in the developing rodent brain, with expression detectable at least as early as embryonic day (E) 13 (Rotwein et al., 1988;

*Corresponding author. Tel.: +1 604 875 2000x5095; fax: +1 604 875 3597. E-mail address: jrokusky@interchange.ubc.ca (J.R. O'Kusky).

Ayer-Le Lievre et al., 1991). Both IGF-I and its transmembrane receptor, the type 1 IGF receptor, are expressed in the embryonic and postnatal rodent cerebral cortex, with peak expression occurring between postnatal day (P) 0 and P28 (Ayer-Le Lievre et al., 1991; Bach et al., 1991; Bondy, 1991; Bondy et al., 1992).

Multiple lines of evidence indicate that IGF-I is capable of stimulating brain growth. Analyses of transgenic (Tg) mice, in which IGF-I is overexpressed in the brain, indicate that IGF-I acts to increase brain weight and volume (Gutierrez-Ospina et al., 1996; Ye et al., 1996; Dentremont et al., 1999; O'Kusky et al., 2000; Popken et al., 2004; Hodge et al., 2005). A number of *in vitro* studies indicate that IGF-I promotes precursor proliferation of both neurons (Lenoir and Honegger, 1983; DiCicco-Bloom and Black, 1988; Drago et al., 1991; Arsenijevic et al., 2001) and oligodendrocytes (McMorris and Dubois-Dalcq, 1988; Mozell and McMorris, 1991). Increased neuron progenitor proliferation in the cerebral cortex stimulated by IGF-I also has been demonstrated *in vivo*. In mice that overexpress IGF-I from early in embryonic development under the control of nestin genomic regulatory elements, called nestin/IGF-I transgenic (Tg) mice, the total number of neurons in the cerebral cortex is increased during embryonic life (Popken et al., 2004), as a result of a shorter cell cycle length and an increased rate of re-entry of progenitors into the mitotic cell cycle during cortical neurogenesis (Hodge et al., 2004).

Both *in vitro* and *in vivo* studies (Aizeman and De Vellis, 1987; Torres-Aleman et al., 1990a,b; Bozyczko-Coyne et al., 1993; Russell and Feldman, 1999; Takadera et al., 1999; Chrysis et al., 2001; Yamada et al., 2001; Popken et al., 2004) also demonstrate that IGF-I promotes cell survival through its anti-apoptotic actions. The extent to which an IGF-I-mediated inhibition of apoptosis modulates neuron number is not known. We, therefore, evaluated apoptosis during development in nestin/IGF-I Tg mice. In this line of Tg mice the pattern of IGF-I overexpression is similar to the normal pattern of IGF-I expression in the brain (Rotwein et al., 1988) in that transgene expression begins during embryonic development, rises to a peak at P5–P10 and then decreases to a steady-state level by P20 (Popken et al., 2004).

2. Materials and methods

Nestin/IGF-I Tg mice were generated at the University of North Carolina at Chapel Hill as described previously (Popken et al., 2004). These Tg mice carried a transgene composed of regulatory regions of the human nestin gene, including the second intron of this gene, in combination with the minimal promoter of the herpes simplex virus immediate early gene ICP4, human IGF-IA cDNA, a signal sequence from rat somatostatin and polyadenylation signals derived from the human growth hormone gene (Popken et al., 2004). Mice used in the present studies were generated by breeding male heterozygous Tg mice with normal non-Tg C57BL/6 female mice (Charles River Laboratories, Wilmington, MA). Litters derived from these matings typically consisted of 50% Tg and 50% normal non-transgenic littermate control mice. Tg mice were routinely identified by PCR of tail genomic DNA. All animal procedures were conducted in accordance with guidelines specified by institutional review committees of the University of British Columbia and the University of North Carolina at Chapel Hill. Efforts were made to optimize experimental design so as to minimize the number of animal subjects used and to alleviate pain and suffering.

Detailed analyses of the expression pattern of the nestin/IGF-I transgene have been reported in a previous study (Popken et al., 2004). Briefly, expression of the nestin/IGF-I transgene was evident in the CNS by as early as E13. At this time, the transgene was expressed in a number of brain regions including the ventricular zone (VZ) of the developing cerebral wall, and expression later became apparent in the cortical plate. During postnatal development, transgene

expression was noted to be relatively homogenous throughout the cerebral cortex (Popken et al., 2004).

2.1. Tissue collection

E16 embryos were obtained by hysterotomy from timed-pregnant dams after deep anesthesia induced by intraperitoneal (i.p.) injections of ketamine (Ketalean, 100 mg/kg; Bimeda-MTC Animal Health Inc., Cambridge, Ontario, Canada) and xylazine (Rompun, 10 mg/kg; Bayer Inc., Toronto, Ontario, Canada). Heads were fixed overnight by immersion in 70% ethanol at 4 °C, and embedded in paraffin. Serial sections were cut at a thickness of 20 μm in the coronal plane through the cerebral hemispheres and mounted individually on Colorfrost Plus glass slides (Fisher Scientific, Ottawa, Ontario, Canada).

Mice at P0, P5 and P270 were anesthetized as described above and perfused through either the left ventricle (P0, P5) or the ascending aorta (P270) with a fixative solution containing 4% paraformaldehyde in 0.1 M phosphate buffer (pH 7.4) for 30 min at perfusion pressures of 50–60 mmHg (P0), 60–70 mmHg (P5) or 100–110 mmHg (P270). Brains were weighed following removal from the skull and post-fixed in additional fixative solution for 40 min (P0, P5) or for 24 h at 4 °C. Individual brains were cryoprotected by immersion in 30% sucrose in 0.1 M phosphate buffer overnight at 4 °C. Serial frozen sections were cut at a thickness of 50 μm in the coronal plane through the cerebral hemispheres, and individual sections were mounted on chrome alum coated glass slides. Every fourth section in this series was stained for Nissl substance using 0.1% thionine in acetate buffer (pH 3.7).

2.2. Assessment of apoptosis in the cerebral cortex at E16

Every 10th section through the brain was heated in antigen unmasking solution (Vector Laboratories, Burlingame, CA) in a microwave oven for 10 min. Sections were then incubated with polyclonal rabbit anti-cleaved caspase-3 primary antibody overnight at 4 °C (1:50 dilution; Cell Signaling Technologies, Beverly, MA). This antibody specifically detects cleaved caspase-3 and does not react with inactive forms of caspase-3 (*e.g.* procaspase-3) or with other caspases. Detection of primary antibody binding was accomplished using an ABC Elite Kit (Vector Laboratories) according to the manufacturer's protocol. Sections were counterstained with 0.1% aqueous basic fuchsin (Fisher Scientific). Sections processed without the addition of primary antiserum were used as negative controls.

The areal density of apoptotic cells (N_A, cells/mm^2) in E16 Tg and control embryos ($N = 4$ per group) was determined for the full height of the telencephalic wall, from the ventricular to the pial surfaces. Sections were examined with an Olympus BH-2 compound microscope (10× planapochromatic objective) interfaced to a Bioquant TCW98 image analysis system (R&M Biometrics, Nashville, TN) and viewed at a final magnification of 188×. On each section, the outline of the telencephalic wall corresponding to the cerebral cortex was traced using established boundary criteria (Alvarez-Bolado and Swanson, 1996) and its area was measured in μm^2. Cleaved caspase-3 immunoreactive cells were counted on each section if they fell within the outlined area of the cerebral wall. The number of apoptotic cells/mm^2 was determined as the total number of caspase-3 positive cells across all sections divided by the sum of all area measurements. Mean cellular profile areas were determined for each mouse by measuring the areas of cleaved caspase-3 immunoreactive cells in μm^2, using a 100× oil-immersion planapochromatic objective and viewed at a final magnification of 1880×. For all variables measured at E16, statistical comparisons between control and Tg mice were conducted using Student's *t*-test.

2.3. Assessment of apoptosis in the cerebral cortex at P0 and P5

From the serial frozen sections, every fourth section was processed for the detection of cleaved caspase-3 immunoreactivity by incubating with polyclonal rabbit anti-cleaved caspase-3 primary antiserum (1:1500 dilution) overnight at room temperature. Sections were then incubated in biotinylated goat anti-rabbit IgG secondary antibody (1:200) for 1 h at room temperature. Further processing was carried out using a Vector Elite ABC kit (Vector Laboratories) according to the manufacturer's instructions, with DAB as the chromogen. Sections were mounted on glass slides and lightly counterstained with 0.1% aqueous basic fuchsin. Sections incubated without the addition of primary antiserum were used as negative controls.

The total volume of the cerebral cortex was determined using Cavalieri's direct estimator (Gundersen et al., 1988a). Briefly, sections were examined with a 4× planapochromatic objective at a final magnification of 75×, and the area of the cerebral cortex was traced and measured in μm^2 on each section. The total volume of the cerebral cortex was determined from $V = \Sigma A \times T \times 4$, where ΣA is the sum of all area measurements, T is the section thickness (50 μm), and 4 is the periodicity of the section sample.

The N_V and total number of cleaved caspase-3 immunoreactive cells in the cerebral cortex were determined at P0 and P5 using the optical disector method (Gundersen et al., 1988b). Briefly, sections were examined using a 100× oil-immersion planapochromatic objective at a final magnification of 1880×. A square disector counting frame was focused approximately 3 μm below the section surface and moved through a set distance of section thickness in the *Z*-axis. The dimensions of the disector counting frame were 25 μm × 25 μm × 20 μm, where 20 μm was the distance traveled in the *Z*-axis. Cells that came into focus entirely within the counting frame and those cells that were intersected by the inclusion edges were scored. At least 200–250 cells were counted for each animal. The N_V of immunoreactive cells was calculated from the equation $N_V = \Sigma Q^- / \Sigma V_{Dis}$, where ΣQ^- is the sum of the cells counted and V_{Dis} is the sum of the disector volumes. The disector volume was calculated from $V_{Dis} = a_{Dis} \times h$, where a_{Dis} is the area of the counting frame and h is the distance traveled in the *Z*-axis plane (*i.e.* the disector height). The total number of cleaved caspase-3 immunoreactive cells was calculated for each animal using the estimates of total cortical volume and N_V of caspase-3 immunoreactive cells. For P0 animals, studies were carried out on three animals per group. For P5 animals, studies were carried out on three Tg animals and five control mice. For all variables, statistical comparisons between control and Tg mice were conducted using 2 × 2 (groups × ages) ANOVA.

2.4. N_V and total number of cortical neurons at P0, P5 and P270

Stereological analyses were performed to measure the N_V and total number of neurons in the cerebral cortex of both hemispheres, using the serial sections stained for Nissl substance. Total cortical volume was measured using Cavalieri's direct estimator (Gundersen et al., 1988a), as described above. The N_V of neurons in the cerebral cortex was determined using the optical disector method (Gundersen et al., 1988b). Neuron counts were conducted on seven sections that were equally spaced along the caudal-to-rostral extent of the cerebral hemispheres. On each section, a random set of sampling points was generated over the cerebral cortex (Bioquant TCW98 stereology toolkit, R&M Biometrics). Approximately 15–20 points were sampled per section. Sections were examined at individual points using a 100× oil-immersion planapochromatic objective at a final magnification of 1880×. The disector counting frame measured 15 μm × 15 μm × 10 μm for mice at P0, 25 μm × 25 μm × 10 μm for mice at P5, and 30 μm × 30 μm × 10 μm for mice at P270. At least 200–250 cells were counted for each animal. The total number of neurons in the cerebral cortex was calculated for each animal using the estimates of neuronal N_V and total cortical volume.

3. Results

3.1. Apoptosis in the cerebral wall at E16

Very few apoptotic cells were observed in either Tg or control embryos in the embryonic telencephalic wall corresponding to the primordial cerebral cortex. This paucity of apoptotic cells precluded quantification using the disector method. Nonetheless, the areal density of caspase-3 immunoreactive cells (cells/mm^2 of section surface) could be assessed and was found to be significantly less in Tg embryos as compared to controls (46%, $P < 0.01$). Mean values (±S.E.M.) were 1.048 ± 0.154 cells/mm^2 for Tg embryos and 1.943 ± 0.122 cells/mm^2 for controls, indicating that very few cells were undergoing apoptosis in either group. In both groups, apoptotic cells were observed in all zones of the cerebral wall. However, more apoptotic cells were generally located in the intermediate zone and cortical plate than in the proliferative zones (VZ, SVZ).

The mean profile area of cleaved caspase-3 immunoreactive cells did not differ significantly between groups on E16 ($P > 0.05$). The mean profile area of apoptotic cells was 22.73 ± 0.94 μm^2 for Tg and 23.08 ± 0.36 μm^2 for controls. Because the cell profile areas did not differ significantly between Tg and control embryos, the probability of individual apoptotic cells being intersected by the plane of section was roughly the same in both groups, and thus, these estimates of N_A were not biased by differences in cell size.

3.2. Apoptosis in the cerebral cortex during early postnatal development

Apoptotic cells were observed in all layers and cytoarchitectonic regions of the cerebral cortex in Tg and control mice at P0 and P5. Although the overall density of apoptotic cells was visibly lower in Tg mice at P0, a substantial number of cleaved caspase-3 immunoreactive cells were observed in layer II/III of the cingulate and retrosplenial (agranular and granular) cortices in both groups (Fig. 1). At P5, apoptotic cells were particularly apparent in layer II/III in the cingulate, retrosplenial, frontal and primary motor regions of the cortex in both groups, although they were observed at a lower density in Tg mice. Cleaved caspase-3 immunoreactive cells also were observed in layer V in the primary motor and primary somatosensory regions, and these cells had the morphological appearance of large pyramidal neurons. The general distribution pattern of apoptotic cells within the cerebral cortex was similar in Tg and control mice. Most of the cleaved caspase-3 immunoreactive cells in the cerebral cortex displayed morphological characteristics of neurons, including dendritic arborizations (Fig. 2A and B). Many cells displayed obvious neuronal characteristics, but had degenerated to the point where cellular processes exhibited a distinctly beaded appearance (Fig. 2C). A small proportion of labeled cells (<20%) exhibited short processes or no processes at all, and may have been either apoptotic neurons or glia. In some cases, the labeled cells had degenerated to the point where the cell body and processes were substantially degraded, indicating that apoptosis was quite advanced (Fig. 2D). This type of cellular profile was always scored as a single cell.

The N_V of cleaved caspase-3-immunoreactive cells in the cerebral cortex was analyzed at P0 and P5 using a 2 × 2 ANOVA comparison of Tg and control mice (Table 1). A main effect for groups indicated that the N_V of cleaved caspase-3 immunoreactive cells was decreased by 31–39% in Tg mice ($P < 0.001$). A main effect of ages was also noted ($P < 0.001$), indicating that the N_V of apoptotic cells in the cortex was greater at P0 than at P5. The groups × ages interaction was not significant ($P = 0.07$), so further individual group comparisons were not warranted. Using estimates of the total cortical volume and the N_V of apoptotic cells at P0 and P5, estimates of the total number of apoptotic cells in the cortex were calculated for each mouse. Analysis of the data using 2 × 2 ANOVA showed that the main effect for groups was not significant ($P > 0.05$), indicating that the total number of apoptotic cells in the cortex did not differ between Tg and control mice (Table 1). As well, the main effect for ages was not significant ($P > 0.05$),

indicating that the total number of apoptotic cells in the cerebral cortex did not differ significantly between P0 and P5 (Table 1).

3.3. Cortical volume, neuronal N_V and total neuron number at P0 and P5

The increased expression of IGF-I in nestin/IGF-I transgenic mice resulted in increased brain weight, but no change in body weight at P0 and P5 (Table 1). Stereological analysis of the cerebral cortex revealed significantly greater cortical volume in Tg mice ($P < 0.05$), compared to littermate controls (Table 1). The N_V of neurons in the cerebral cortex did not differ significantly between groups at either age studied ($P > 0.05$). However, analysis of the total number of cortical neurons revealed a significant main effect for groups ($P < 0.001$), indicating that total neuron number was increased in Tg mice. The total number of neurons in the cortex was increased significantly in Tg mice by 29% at both P0 and P5.

3.4. Stereological analyses of the cerebral cortex at nine months of age

Stereological analyses were performed to measure the total volume, N_V of neurons, and total number of neurons in the cerebral cortex of nestin/IGF-I Tg and control mice at nine months of age (Table 2). No signs of gross malformation or pathological abnormalities were apparent in the brains of Tg mice. The brains of nestin/IGF-I Tg mice, however, were visibly larger than those of littermate controls (Fig. 3). Brain weights of Tg mice were significantly greater (41%) than those of control mice, but body weights did not differ significantly between groups (Table 2). The total volume of the cerebral cortex was significantly increased by 26% in Tg mice compared to controls. The N_V of neurons in the cortex did not differ significantly between groups. However, total neuron number was significantly increased by 31% in nestin/IGF-I Tg mice (Table 2), indicating that elevated IGF-I expression in Tg mice persistently augments cortical neuron number into adult life, well beyond the period of naturally occurring neuron death.

4. Discussion

As in previous reports (Srinivasan et al., 1998; DiCunto et al., 2000; Hu et al., 2000; Camarero et al., 2001) this study employed immunohistochemical detection of activated caspase-3 to identify neuronal apoptosis. Caspase-3 is expressed in the developing brain (Srinivasan et al., 1998; De Bilbao et al., 1999), while defects in neuronal apoptosis have been demonstrated in mice lacking the caspase-3 gene (Kuida et al., 1996). The results of the present study demonstrate that elevated *in vivo* IGF-I expression promotes neuron survival in the cerebral cortex during late prenatal and early postnatal development. As a result, the increased number of cells accrued by accelerated proliferation during embryonic life (Hodge et al., 2004) is maintained throughout postnatal life and into the adult. This finding is in agreement with previous studies showing that IGF-I promotes neuron and glia survival *in vitro* (Aizeman and De Vellis, 1987; Torres-Aleman et al., 1990a,b; Pons et al., 1991; Barres et al., 1992; Bozyczko-Coyne et al., 1993; Sortino and Canonico, 1996; Russell and Feldman, 1999; Ye and D'Ercole, 1999; Yamada et al., 2001; Ness et al., 2002; Ness and Wood, 2002). It also is consistent with a previous report showing that IGF-I overexpression during postnatal development reduced the density of apoptotic cells in the cerebellum *in vivo* on P7 by decreasing procaspase-3 and cleaved caspase-3 protein levels in the cerebellum (Chrysis et al., 2001). The current findings, therefore, indicate that the increased neuron number documented in the present study and previously in nestin/IGF-I Tg mice at P12 (Popken et al., 2004; Hodge et al., 2005) results, at least in part, from an IGF-I-mediated enhancement of neuron survival.

In both Tg and control embryos, caspase-3 immunoreactive cells were observed so rarely in the cerebral wall (*i.e.* on average, only 1 or 2 cells/mm^2 of section area, respectively) that unbiased stereological methods could not be used to estimate the N_V of apoptotic cells.

Attempts were made to measure the N_V of apoptotic cells, using the disector method (Gundersen et al., 1988b). However, in both Tg and control embryos, the number of apoptotic cells in the entire cerebral cortex was not sufficient to allow for the use of this method, which requires that at least 200 target cells be counted within representative random disector volumes from each subject. It was found that, on average, the total number of apoptotic cells in the telencephalic wall corresponding to the entire cerebral cortex for a given embryo was substantially less than 200 cells, even if all sections in the series (on average, approximately 135 sections per embryo) were processed for immunohistochemistry. However, differences between groups in our measurements of N_A for caspase-3 immunoreactive cells in the embryonic cerebral cortex likely correlate closely with differences in their N_V. The mean profile area of apoptotic cells did not differ significantly between groups (<2%), and there were no consistent differences between groups in the apparent shape of these cellular profiles. Therefore, apoptotic cells in both groups would have had roughly the same probability of being intersected by the plane of section, and the 46% decrease in N_A observed in Tg embryos likely reflects a similar decrease in N_V.

Augmented IGF-I expression during embryonic development reduces apoptosis by 46% in the developing embryonic cerebral wall, at least at E16. In previous studies of nestin/IGF-I Tg mice, the number of cells in the cortical plate at E16 was shown to be increased by 54% in Tg embryos (Popken et al., 2004). The results of the present analysis indicate that an IGF-I-mediated decrease in apoptosis probably contributes to the increase in cortical plate cell number at E16. We also documented enhanced cell cycle progression and increased cell cycle re-entry in the cerebral wall of these Tg embryos on E14–E15 (Hodge et al., 2004), indicating that elevated IGF-I expression increased cortical plate cell number by stimulating neuron progenitor proliferation during embryonic development of the cortex. The magnitude of apoptotic cell death in neural precursors is a controversial issue, with previous studies showing varying amounts of apoptosis in the embryonic brain. While studies using *in situ* end labeling techniques (ISEL) to identify DNA double strand breaks suggest that 50–70% of the cells in the embryonic cortex are eliminated by apoptosis (Blaschke et al., 1996), other reports, using the TUNEL method, demonstrate that apoptosis is a rare event, with less than 9% of cortical cells undergoing apoptosis on E16 (Thomaidou et al., 1997). The current findings are consistent with analyses showing that a relatively small number of cells undergo apoptosis in the embryonic cortex (Thomaidou et al., 1997; Verney et al., 2000).

IGF-I overexpression in Tg mice during postnatal development significantly decreases the N_V of apoptotic cells on P0 and P5 by 30–40%, as judged using an antibody that specifically detects activated caspase-3. This reduction in the N_V of apoptotic cells was slightly greater in Tg mice at P5 (39%) than at P0 (31%). At these postnatal ages, the N_V of cortical neurons does not differ significantly between groups, indicating that the density of neurons in the cortex is similar in both Tg and control mice. The documented reduction in the N_V of apoptotic cells in the cortex, without a parallel change in the N_V of cortical neurons, therefore, corresponds to a substantial decrease in the proportion of cells undergoing apoptosis in the cerebral cortex of Tg mice. At the time of perfusion, approximately 68 cells per 100,000 on average were observed to be undergoing apoptosis in control mice, while only 42 per 100,000 were apoptotic in Tg mice. Given the significantly greater volume of the cerebral cortex in Tg mice, the total number of apoptotic cells did not differ significantly.

This decrease in the proportion of apoptotic neurons in the cerebral cortex of Tg mice is not likely due to increased brain growth, where a fixed number of apoptotic neurons is contained in a larger population of cortical neurons, resulting from accelerated mitosis at earlier stages of embryonic development. Neuronal apoptosis during the phase of programmed cell death in early postnatal development is thought to be a mechanism for matching a population of projection neurons to the size of its target field, and to be precipitated by inadequate

neurotrophic support *via* decreased retrograde transport of growth factors from the target (for reviews, see Cowan et al., 1984; Oppenheim, 1991; Burek and Oppenheim, 1996). In many regions of the central nervous system, typically half of the neurons that are initially generated through mitosis of precursors in a proliferative zone will degenerate at some point between their migration into that specific region and their final maturation as distinguished by axon outgrowth, synaptogenesis and myelination. However, the proportion of neurons undergoing programmed cell death can vary substantially depending on the size of the target field. Numerous studies have shown that full or partial ablation of the target will increase the proportion of apoptotic neurons, while a supernumerary target (*i.e.* increased tissue volume, increased numbers of neurons or muscle fibers) will decrease the proportion of apoptotic neurons in the source region (Cowan et al., 1984). In nestin/IGF-I Tg mice, increased regional tissue volumes and increased neuron numbers have been observed throughout the telencephalon and diencephalon (Popken et al., 2004). There would appear to be little or no mismatch between cortical neurons and their targets within these regions (*i.e.* callosal, cortico-cortical, corticostriate, corticothalamic projections), and one would expect to see similar proportions of apoptotic neurons in Tg and control mice. Given the caudal-to rostral gradient in neurogenesis in the central nervous system and the fact that the nestin/IGF-I transgene in these Tg mice begins expression at E13, one might expect to see a mismatch between cortical neurons and their relatively smaller targets in the brainstem and spinal cord. However, a relative reduction in target size in these regions would be expected to produce an increased proportion of apoptotic cortical neurons in Tg mice, corresponding to corticobulbar and corticospinal projections. The significant reduction in the proportion of apoptotic neurons observed in the cerebral cortex of these Tg mice does not seem to result from simple brain growth. Rather, the anti-apoptotic effects of elevated IGF-I in these Tg mice most likely result from a direct inhibition of apoptosis mediated through Bcl-2 family proteins, which include both anti-apoptotic (Bcl-2, Bcl-X_L) and pro-apoptotic (Bad, Bax, Bim) members. Previous *in vitro* and *in vivo* studies have shown that elevated levels of IGF-I act to reduce neuronal apoptosis by increasing expression of Bcl-2 and Bcl-X_L (Chrysis et al., 2001) and decreasing expression of Bad, Bax and Bim (Gleichmann et al., 2000; Chrysis et al., 2001; Linseman et al., 2002), leading to decreased activation of caspase-9 and caspase-3 (Takadera et al., 1999; Chrysis et al., 2001; Linseman et al., 2002; Vincent et al., 2004; Zhong et al., 2004).

Neuron apoptosis was more prevalent in the cerebral cortex during early postnatal development than during embryonic development in both Tg and control mice, consistent with a number of other studies (Thomaidou et al., 1997; Verney et al., 2000; Spreafico et al., 1995). The peak time of cortical neuron apoptosis documented in the present study differs somewhat from other reports of cortical apoptosis in rodents. We found that the N_V of apoptotic neurons was greater at P0 than at P5 in both groups. Other studies have shown low levels of apoptosis in the mouse cortex at birth, with apoptosis peaking at approximately P4 (Verney et al., 2000). Similarly, the peak of neuron apoptosis in the cerebral cortex of rats has been shown to occur between P5 and P8 (Spreafico et al., 1995). It is possible that these discrepancies among reports may be explained by differences in the locations where apoptotic cells were counted. For example, the data of Verney et al. (2000) were confined to multiple regions of the parietal cortex, whereas the analysis reported here encompassed all cytoarchitectonic regions of the cortex. In both Tg and control mice, the density of apoptotic cells was lowest at E16, rose to a peak at P0, and declined thereafter. These data indicate that, while IGF-I decreases the density of apoptotic neurons during postnatal development, the temporal pattern of apoptosis in the cortex is not altered in Tg mice.

Transgene expression in nestin/IGF-I Tg mice decreases to a steady-state level by P20 (Popken et al., 2004), raising the possibility that decreased transgene expression in these Tg mice may increase their rate of neuronal apoptosis in the cerebral cortex during later stages of development. To address this issue, stereological analyses of the cerebral cortex were

performed in adult Tg and control mice at nine months of age (P270), well after the time when transgene expression reaches steady-state levels. Our data indicate that neurons are not eliminated in Tg mice during later phases of postnatal development, and that IGF-I does not merely reduce the rate of elimination for normally extraneous cortical neurons. The N_V of neurons did not differ between nestin/IGF-I Tg and control mice at P270, or at any age in this study. In both groups the N_V of neurons decreased at successive ages, from approximately 600,000 at P0 to 180,000 at P270, as dendritic outgrowth and axon formation increased both the volume of tissue and distance between neuronal cell bodies. A number of studies have shown that increased expression of IGF-I in different lines of mice during postnatal development results in decreased neuronal N_V and increased process outgrowth in various regions of the brain (Gutierrez-Ospina et al., 1996; Dentremont et al., 1999; O'Kusky et al., 2000). The current results, therefore, suggest that elevated IGF-I expression in nestin/IGF-I Tg mice does not augment process outgrowth sufficiently to reduce neuronal packing density. This is likely due to the fact that peak transgene IGF-I in nestin/IGF-I Tg mice occurs during late embryonic and early postnatal development, before extensive process outgrowth has occurred. Alternatively, the cellular sites of IGF-I transgene expression in nestin/IGF-I Tg mice may limit the availability of IGF-I at outgrowing processes. In any case, this finding clearly differentiates nestin/IGF-I Tg mice from previously studied lines of IGF-I Tg mice.

The results of the present study indicate that IGF-I promotes neuron survival in the cerebral cortex during embryonic and early postnatal development by decreasing the numerical density and proportion of activated caspase-3 immunoreactive apoptotic neurons. These results demonstrate that increased neuron number in the cerebral cortex of nestin/IGF-I Tg mice results from both enhanced neuron progenitor proliferation primarily during embryonic development (Hodge et al., 2004) and decreased neuron apoptosis primarily during early postnatal development, and that this increase in neuron number is sustained in the adult brain.

Acknowledgements

This study was supported by grant MOP37536 from the CIHR/Canadian Neurotrauma Research Program (JRO) and grant HD08299 from NICHD (AJD).

Abbreviations

ANOVA
: analysis of variance

N_A
: areal density (cells/mm^2)

E
: embryonic day

IGF-I
: insulin-like growth factor-I

i.p
: intraperitoneal

N_V
: numerical density (cells/mm^3)

P
: postnatal day

SVZ

subventricular zone

Tg

transgenic

VZ

ventricular zone

References

Aizeman Y, De Vellis J. Brain neurons develop in a serum and glia free environment: effects of transferrin, insulin, insulin-like growth factor-I and thyroid hormones on survival, growth and differentiation. Brain Res 1987;406:32–42. [PubMed: 3105814]

Alvarez-Bolado, G.; Swanson, LW. Developmental Brain Maps: Structure of the Embryonic Rat Brain. Elsevier Science Publishing; New York: 1996.

Arsenijevic Y, Weiss S, Schneider B, Aebischer P. Insulin-like growth factor-I is necessary for neural stem cell proliferation and demonstrates distinct actions of epidermal growth factor and fibroblast growth factor-2. J Neurosci 2001;21:7194–7202. [PubMed: 11549730]

Ayer-Le Lievre C, Stahlbom PA, Sara VR. Expression of IGF-I and -II mRNA in the brain and craniofacial region of the rat fetus. Development 1991;111:105–115. [PubMed: 2015788]

Bach MA, Shen-Orr Z, Lower WL, Roberts CT, LeRoith D. Insulin-like growth factor-I mRNA levels are developmentally regulated in specific regions of the brain. Mol Brain Res 1991;10:43–48. [PubMed: 1647481]

Barres BA, Hart IK, Coles HS, Burne JF, Voyvodic JT, Richardson WD, Raff MC. Cell death and control of cell survival in the oligodendrocyte lineage. Cell 1992;70:31–46. [PubMed: 1623522]

Blaschke AJ, Staley K, Chun J. Widespread programmed cell death in the proliferative and postmitotic regions of the fetal cerebral cortex. Development 1996;122:1165–1174. [PubMed: 8620843]

Bondy CA. Transient IGF-I gene expression during the maturation of functionally related central projection neurons. J Neurosci 1991;11:3442–3455. [PubMed: 1658250]

Bondy C, Werner H, Roberts CT Jr, LeRoith D. Cellular pattern of type-I insulin-like growth factor receptor gene expression during maturation of the rat brain: comparison with insulin-like growth factors I and II. Neuroscience 1992;46:909–923. [PubMed: 1311816]

Bozyczko-Coyne D, Glicksman MA, Prantner JE, McKenna B, Connors T, Friedman C, Dasgupta M, Neff T. IGF-I supports the survival and/or differentiation of multiple types of central nervous system neurons. Ann N Y Acad Sci 1993;692:311–313. [PubMed: 8215039]

Burek MJ, Oppenheim RW. Programmed cell death in the developing nervous system. Brain Pathol 1996;6:427–446. [PubMed: 8944315]

Camarero G, Avendano C, Fernandez-Moreno C, Villar A, Contreras J, de Pablo F, Pichel JG, Varela-Nieto I. Delayed inner ear maturation and neuronal loss in postnatal Igf-1-deficient mice. J Neurosci 2001;21:7630–7641. [PubMed: 11567053]

Chrysis D, Calikoglu AS, Ye P, D'Ercole AJ. Insulin-like growth factor-I overexpression attenuates cerebellar apoptosis by altering the expression of Bcl family proteins in a developmentally specific manner. J Neurosci 2001;21:1481–1489. [PubMed: 11222638]

Cowan WM, Fawcett JW, O'Leary DDM, Stanfield BB. Regressive events in neurogenesis. Science 1984;225:1258–1265. [PubMed: 6474175]

De Bilbao F, Guarin E, Nef P, Vallet P, Giannakopoulos P, Dubois-Dauphin M. Postnatal distribution of cpp32/caspase 3 mRNA in the mouse central nervous system: an in situ hybridization study. J Comp Neurol 1999;409:339–357. [PubMed: 10379822]

Dentremont KD, Ye P, D'Ercole AJ, O'Kusky JR. Increased insulin-like growth factor-I (IGF-I) expression during early postnatal development differentially increases neuron number and growth in medullary nuclei of the mouse. Dev Brain Res 1999;114:135–141. [PubMed: 10209251]

DiCicco-Bloom E, Black IB. Insulin-like growth factors regulate the mitotic cycle in cultured rat sympathetic neuroblasts. Proc Natl Acad Sci USA 1988;85:4066–4070. [PubMed: 2897692]

DiCunto F, Imarisio S, Hirsch E, Broccoli V, Bulfone A, Migheli A, Atorzi C, Turco E, Triolo R, Dotto GP, Silengo L, Altruda F. Defective neurogenesis in citron kinase knockout mice by altered cytokinesis and massive apoptosis. Neuron 2000;28:115–127. [PubMed: 11086988]

Drago J, Murphy M, Carroll SM, Harvey RP, Bartlett PF. Fibroblast growth factor-mediated proliferation of central nervous system precursors depends on endogenous production of insulin-like growth factor I. Proc Natl Acad Sci USA 1991;88:2199–2203. [PubMed: 2006157]

Gleichmann M, Weller M, Schultz JB. Insulin-like growth factor-I-mediated protection from neuronal apoptosis is linked to phosphorylation of the pro-apoptotic protein BAD but not to inhibition of cytochrome c translocation in rat cerebellar neurons. Neurosci Lett 2000;282:69–72. [PubMed: 10713398]

Gundersen HJG, Bendtsen TF, Korbo L, Marcussen N, Moller A, Nielsen K, Nyengaard JR, Pakkenberg B, Sorensen FB, Vesterby A, West MJ. Some new, simple and efficient stereological methods and their use in pathological research and diagnosis. APMIS 1988a;96:379–394. [PubMed: 3288247]

Gundersen HJG, Bagger P, Bendtsen TF, Evans SM, Korbo L, Marcussen N, Moller A, Nielsen K, Nyengaard JR, Pakkenberg B, Sorensen FB, Versterby A, West MJ. The new stereological tools: disector, fractionator, nucleator and point sampled intercepts and their use in pathological research and diagnosis. APMIS 1988b;96:857–881. [PubMed: 3056461]

Gutierrez-Ospina G, Calikoglu AS, Ye P, D'Ercole AJ. *In vivo* effects of insulin-like growth factor I on the development of sensory pathways: analysis of the primary somatic sensory cortex (S1) of Tg mice. Endocrinology 1996;137:5484–5492. [PubMed: 8940375]

Hodge RD, D'Ercole AJ, O'Kusky JR. Insulin-like growth factor-I accelerates the cell cycle by decreasing G1 phase length and increases cell cycle reentry in the embryonic cerebral cortex. J Neurosci 2004;24:10201–10210. [PubMed: 15537892]

Hodge RD, D'Ercole AJ, O'Kusky JR. Increased expression of insulin-like growth factor-I (IGF-I) during embryonic development produces neocortical overgrowth with differentially greater effects on specific cytoarchitectonic areas and cortical layers. Dev Brain Res 2005;154:227–237. [PubMed: 15707676]

Hu BR, Lin CL, Ouyang Y, Blomgren K, Siesjo BK. Involvement of caspase-3 in cell death after hypoxia-ischemia declines during brain maturation. J Cereb Blood Flow Metab 2000;20:1294–1300. [PubMed: 10994850]

Kuida K, Zheng TS, Na S, Kuan CY, Yang D, Karasuyama H, Rakic P, Flavell RA. Decreased apoptosis in the brain and premature lethality in cpp32-deficient mice. Nature 1996;384:368–372. [PubMed: 8934524]

Lenoir D, Honegger P. Insulin-like growth factor I (IGF-I) stimulates DNA synthesis in fetal rat brain cell cultures. Exp Brain Res 1983;7:205–213.

Linseman DA, Phelps RA, Bouchard RJ, Le SS, Laessig TA, McClure ML, Heidenreich KA. Insulin-like growth factor-I blocks Bcl-2 interacting mediator of cell death (Bim) induction and intrinsic death signaling in cerebellar granule neurons. J Neurosci 2002;22:9287–9297. [PubMed: 12417654]

McMorris FA, Dubois-Dalcq M. Insulin-like growth factor I promotes cell proliferation and oligodendroglial commitment in rat glial progenitor cells developing *in vitro*. J Neurosci Res 1988;21:199–209. [PubMed: 3216421]

Mozell RL, McMorris FA. Insulin-like growth factor I stimulates oligodendrocyte development and myelination in rat brain aggregate cultures. J Neurosci Res 1991;30:382–390. [PubMed: 1665869]

Ness JK, Mitchell NE, Wood TL. IGF-I and NT-3 signaling pathways in developing oligodendrocytes: differential regulation and activation of receptors and the downstream effector Akt. Dev Neurosci 2002;24:437–445. [PubMed: 12666655]

Ness JK, Wood TL. Insulin-like growth factor I, but not neurotrophin-3, sustains Akt activation and provides long-term protection of immature oligodendrocytes from glutamate-mediated apoptosis. Mol Cell Neurosci 2002;20:476–488. [PubMed: 12139923]

O'Kusky JR, Ye P, D'Ercole AJ. Insulin-like growth factor-I promotes neurogenesis and synaptogenesis in the hippocampal dentate gyrus during postnatal development. J Neurosci 2000;20:8435–8442. [PubMed: 11069951]

Oppenheim RW. Cell death during development of the nervous system. Ann Rev Neurosci 1991;14:453–501. [PubMed: 2031577]

Pons S, Rejas MT, Torres-Aleman I. Ontogeny of insulin-like growth factor I, its receptor, and its binding proteins in the rat hypothalamus. Dev Brain Res 1991;62:169–175. [PubMed: 1722739]

Popken GJ, Hodge RD, Ye P, Zhang J, Ng W, O'Kusky JR, D'Ercole AJ. *In vivo* effects of insulin-like growth factor-I (IGF-I) on prenatal and early postnatal development of the central nervous system. Eur J Neurosci 2004;19:2056–2068. [PubMed: 15090033]

Rotwein P, Burgess SK, Milbrandt JD, Krause JE. Differential expression of insulin-like growth factor genes in rat central nervous system. Proc Natl Acad Sci USA 1988;85:265–269. [PubMed: 3422422]

Russell JW, Feldman EL. Insulin-like growth factor-I prevents apoptosis in sympathetic neurons exposed to high glucose. Horm Metab Res 1999;31:90–96. [PubMed: 10226787]

Sortino MA, Canonico PL. Neuroprotective effect of insulin-like growth factor I in immortalized hypothalamic cells. Endocrinology 1996;137:1418–1422. [PubMed: 8625919]

Spreafico R, Frasson C, Arcelli P, Selvaggio M, De Biasi S. *In situ* labeling of apoptotic cell death in the cerebral cortex and thalamus of rats during development. J Comp Neurol 1995;363:281–295. [PubMed: 8642075]

Srinivasan A, Roth KA, Sayers RO, Shindler KS, Wong AM, Fritz LC, Tomaselli KJ. *In situ* immunodetection of activated caspase-3 in apoptotic neurons in the developing nervous system. Cell Death Differen 1998;5:1004–1016.

Takadera T, Matsuda I, Ohyashiki T. Apoptotic cell death and caspase-3 activation induced by *N*-methyl-D-aspartate receptor antagonists and their prevention by insulin-like growth factor I. J Neurochem 1999;73:548–556. [PubMed: 10428050]

Thomaidou D, Mione MC, Cavanagh JFR, Parnavelas JG. Apoptosis and its relation to the cell cycle in the developing cerebral cortex. J Neurosci 1997;17:1075–1085. [PubMed: 8994062]

Torres-Aleman I, Naftolin F, Robbins RJ. Trophic effects of basic fibroblast growth factor on fetal rat hypothalamic cells: interactions with insulin-like growth factor I. Dev Brain Res 1990a;52:253–257. [PubMed: 2331793]

Torres-Aleman I, Naftolin F, Robbins RJ. Trophic effects of insulin-like growth factor-I on fetal rat hypothalamic cells in culture. Neuroscience 1990b;35:601–608. [PubMed: 2199843]

Verney C, Takahashi T, Bhide PG, Nowakowski RS, Caviness VS Jr. Independent controls for neocortical neuron production and histogenetic cell death. Dev Neurosci 2000;22:125–138. [PubMed: 10657705]

Vincent AM, Mobley BC, Hiller A, Feldman EL. IGF-I prevents glutamate-induced motor neuron programmed cell death. Neurobiol Dis 2004;16:407–416. [PubMed: 15193297]

Yamada M, Tanabe K, Wada K, Shimoke K, Ishikawa Y, Ikeuchi T, Koizumi S, Hatanaka H. Differences in survival-promoting effects and intracellular signaling properties of BDNF and IGF-I in cultured cerebral cortical neurons. J Neurochem 2001;78:940–951. [PubMed: 11553668]

Ye P, Xing YZ, Dai ZH, D'Ercole AJ. *In vivo* actions of insulin-like growth factor-I (IGF-I) on cerebellum development in Tg mice: evidence that IGF-I increases proliferation of granule cell progenitors. Dev Brain Res 1996;95:44–54. [PubMed: 8873975]

Ye P, D'Ercole AJ. Insulin-like growth factor-I protects oligodendrocytes from tumor necrosis factor-α-induced injury. Endocrinology 1999;140:3063–3072. [PubMed: 10385398]

Zhong J, Deng J, Huang S, Yang X, Lee WH. High K+ and IGF-1 protect cerebellar granule neurons via distinct signaling pathways. J Neurosci Res 2004;75:794–806. [PubMed: 14994340]

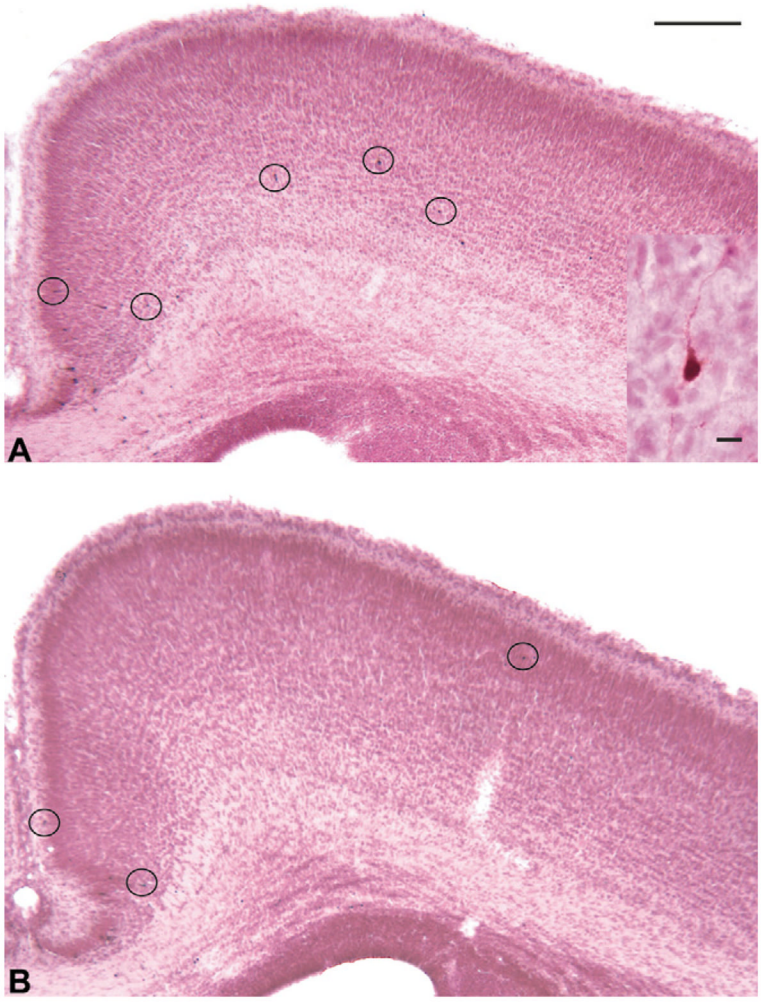

Fig. 1.

Representative photomicrographs illustrating the distribution of cleaved caspase-3 immunoreactive cells in the cerebral cortex of control (A) and nestin/IGF-I Tg (B) mice at P0. The distribution of individual cleaved caspase-3 immunoreactive cells is demonstrated by circles outlining individual cells. The middle caspase-3 immunoreactive neuron in the control cortex (A) is illustrated at greater magnification in the inset. Sections are counterstained with basic fuchsin. Scale bar = 250 μm; scale bar in inset = 10 μm.

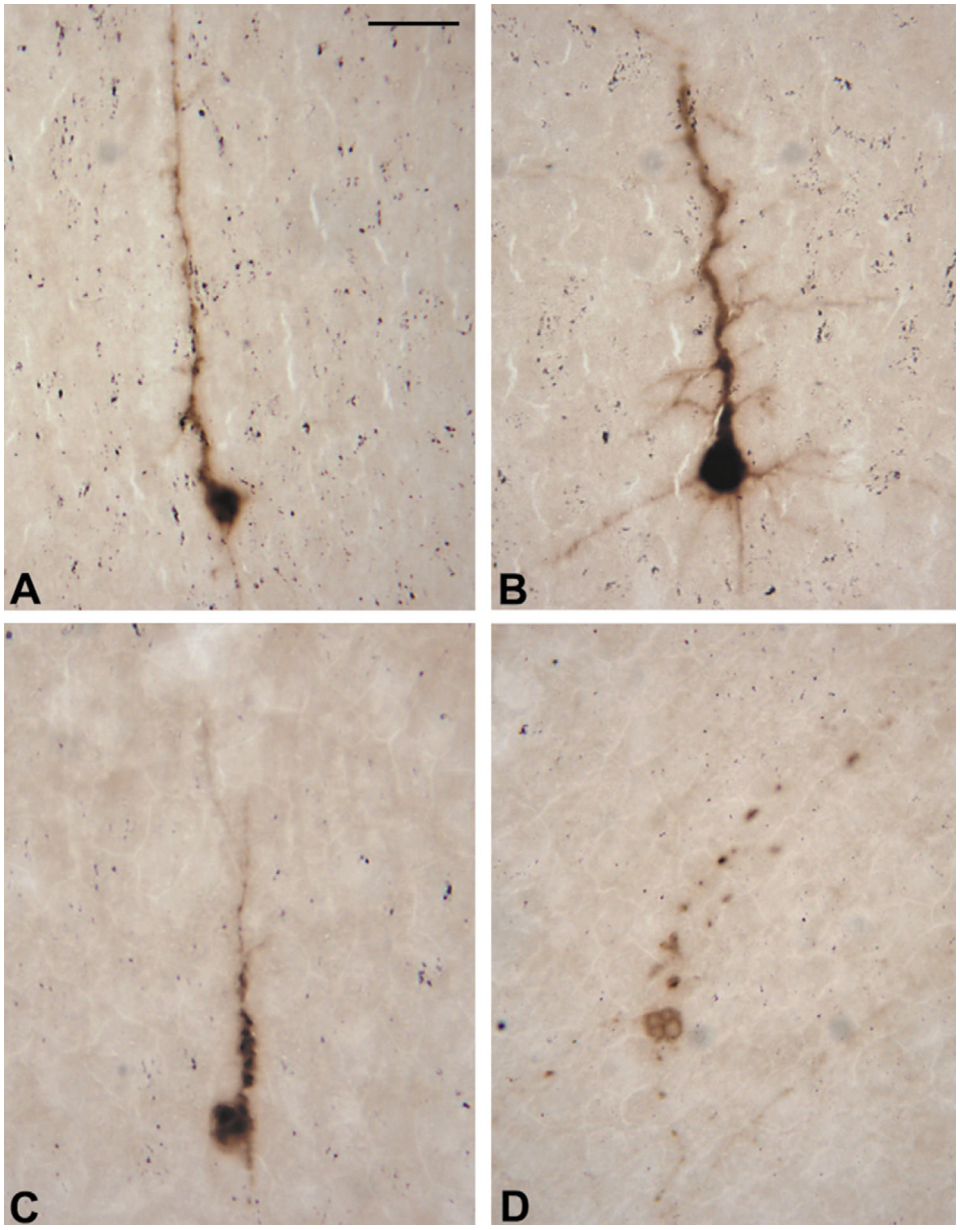

Fig. 2.

Photomicrographs of cleaved caspase-3 immunoreactive cells in the cerebral cortex at P5. These sections were processed without counterstaining to enhance photographic contrast. Some cleaved caspase-3 immunoreactive cells in the cerebral cortex at P0 and P5 exhibited morphological hallmarks that were characteristic of neurons (see A and B), including extensive dendritic arborizations. Other cells exhibited obvious neuronal characteristics, but exhibited degeneration as evidenced by the disintegration of their processes (C). Yet other labeled cells were observed, in which apoptosis appeared to be more advanced (D). These cells were characterized by condensed cell bodies and more severely fragmented processes. Scale bar in A = 10 μm and applies to all panels of the figure.

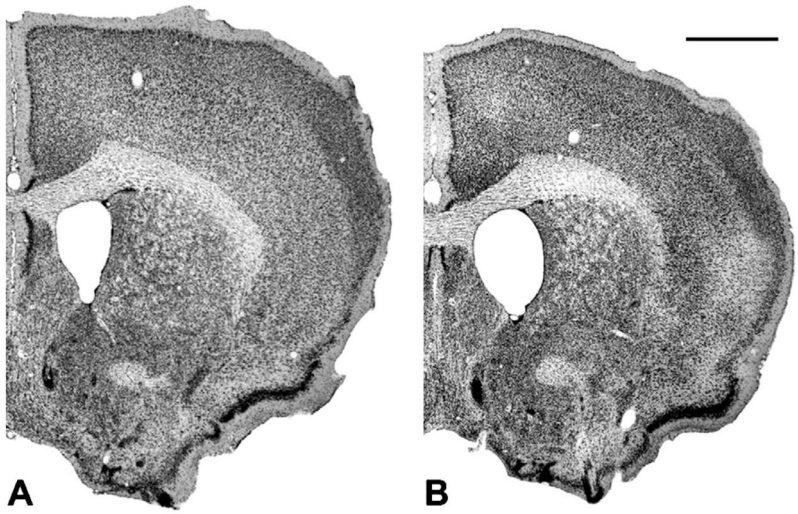

Fig. 3.

Representative sections (30 μm thick), stained with thionine for Nissl substance, through the cerebral hemispheres of nestin/IGF-I Tg (A) and non-Tg littermate control (B) mice at nine months of age (P270). Note the increased size of the cerebral cortex in Tg mice with no apparent difference in the packing of neurons. Scale bar = 1 mm.

Table 1

Summary of morphometric variables for the cerebral cortex measured in nestin/IGF-I transgenic (Tg) and control mice at postnatal day 0 and postnatal day 5

	Postnatal day 0		Postnatal day 5	
	Control	Nestin/IGF-I Tg	Control	Nestin/IGF-I Tg
Brain weight (mg)	77 ± 3	107 ± 3**	161 ± 6	186 ± 7**
Body weight (g)	1.29 ± 0.10	1.39 ± 0.05	3.14 ± 0.26	2.52 ± 0.16
Cortical volume (mm^3)	13.484 ± 0.702	17.576 ± 1.158*	38.245 ± 1.985	43.187 ± 1.195*
N_V of neurons (neurons/mm^3)	611,546 ± 14,694	604,068 ± 8036	275,512 ± 20,696	311,897 ± 26,393
Total number of neurons	8,228,041 ± 285,864	10,608,325 ± 638,927***	10,397,285 ± 351,864	13,407,626 ± 775,809***
N_V caspase-3^+ (cells/mm^3)	430.73 ± 18.39	297.45 ± 8.09***	184.66 ± 12.34	112.29 ± 19.13***
Total caspase-3^+ cell number	5827 ± 500	5217 ± 288	7099 ± 696	4891 ± 972

All values are listed as the mean ± S.E.M. Volume, N_V of neurons, and total number of neurons were measured bilaterally.

* $P < 0.05$ for comparisons between Tg and control mice using 2 × 2 ANOVA.

** $P = 0.001$ for comparisons between Tg and control mice using 2 × 2 ANOVA.

*** $P < 0.001$ for comparisons between Tg and control mice using 2 × 2 ANOVA.

Table 2

Summary of morphometric variables measured in the cerebral cortex in nestin/IGF-I transgenic (Tg) and normal littermate control mice at nine months of age (P270)

	Control	Nestin/IGF-I Tg
Body weight (g)	35.8 ± 5.9	33.6 ± 6.4
Brain weight (mg)	441 ± 10	622 ± 21*
Cortical volume (mm^3)	78.45 ± 3.33	99.01 ± 3.63*
N_V of neurons (neurons/mm^3)	181,228 ± 6976	188,423 ± 7139
Total number of neurons	14,175,559 ± 616,481	18,632,857 ± 852,892*

All values are listed as mean ± S.E.M. Volume, N_V of neurons, and total number of neurons were measured bilaterally.

* $P < 0.01$ for comparisons between Tg and control mice using Student's *t*-test.